



Contents lists available at ScienceDirect

Quaternary International

journal homepage: [www.elsevier.com/locate/quaint](http://www.elsevier.com/locate/quaint)

## Luminescence dating of late holocene dunes showing remnants of early settlement in Cuddalore and evidence of monsoon activity in south east India

Alexander Kunz <sup>a,b,\*</sup>, Manfred Frechen <sup>b</sup>, Ramachandran Ramesh <sup>c</sup>, Brigitte Urban <sup>a</sup>

<sup>a</sup> *Leuphana University, Suderburg, Germany*

<sup>b</sup> *Leibniz Institute for Applied Geophysics, Hannover, Germany*

<sup>c</sup> *Institute for Ocean Management, Anna University, Chennai, India*

### ARTICLE INFO

Article history:

Available online xxx

### ABSTRACT

In this study dunes from south east India were dated using optically stimulated luminescence (OSL) to reconstruct the depositional history. A belt of dunes has developed parallel to the coast between Pondicherry and Karikal in Tamil Nadu, south east India. In the area between Cuddalore and Porto Novo the dune belt is 5 km wide. A transect from the coast to the most western dune inland was investigated. Changes in the environmental conditions are recorded in the dunes. They show features including unconformities, changes in the direction of bedding, erosional features, water escape structures and remnants of human settlements. The OSL results show that strong changes in the environmental conditions occurred about 100 and 300 years ago. The latter event marks also the termination of settlement in this place. The settlement period started about 1500 years previously. The periods of sand mobility and stabilisation of the land surface by soil formation correlate with changes in the precipitation record of India. The investigated dunes very likely reflect fluctuations in the monsoon activity during the last 3500 years in south east India.

© 2009 Elsevier Ltd and INQUA. All rights reserved.

### 1. Introduction

Optically stimulated luminescence (OSL) dating is an excellent tool to determine the deposition age of sediments, which is the time elapsed since the last exposure of the mineral grains to sunlight. OSL dating has been applied to a variety of different depositional environments such as aeolian deposits (e.g., Bateman et al., 2004; Roberts, 2008), fluvial deposits (e.g., Rittenour, 2008; Rodnight et al., 2006) and glacial deposits (e.g., Bateman, 2008; Fuchs and Owen, 2008).

Due to the physical mechanism of the OSL method, reliable and precise results for well bleached aeolian loess or dunes can be determined. Jacobs (2008), Lancaster (2008) and Singhvi and Porat (2008) give summaries of the application of OSL dating to coastal and marine sediments, the development and the dynamics of desert dunes, and geomorphological and palaeoclimatological research in dry lands.

In India, large dune fields occur only in the Thar Desert situated in the northwestern part of Rajasthan, close to the border with

Pakistan. Along the eastern coast of peninsular India, narrow belts of sand dunes, coastal dunes and beach ridges are present (Fig. 1). They are connected to the low lying deltaic and coastal plains. Larger areas covered with dunes are located along the coast of West Bengal in the northeast of India, along the coast of Andhra Pradesh in the delta plains of the Krishna River and the Godavari River, and along the coast of Tamil Nadu in the southeast, especially in the area of the Cauvery Delta and the southeastern-most part along the coast of the Gulf of Mannar. On the west coast of India, beach ridges and dunes occur only in a narrow belt along the south coast of Kerala. Jayappa and Vijaya Kumar (2006) summarize the morphological features of the coast of India.

Luminescence dating was applied on dunes in the Thar Desert (Chawla et al., 1992; Juyal et al., 2003; Singhvi et al., 1994; Singhvi et al., 1982; Thomas et al., 1999) to investigate the sedimentary dynamics of dunes, sand accumulation rates, and palaeoclimate reconstruction. The chronology of dunes in the low lying deltaic and coastal plains in India has not yet been investigated. Sedimentology and mineralogy of the dunes and beach ridges in the region between Pondicherry and Porto Novo (Fig. 2) have been studied to find resources for heavy minerals (Chandrasekharan and Murugan, 2001; Mohan, 1995; Mohan and Rajamanickam, 2000). This study presents the first OSL ages for the dunes in the Cuddalore region. This geochronological framework is used to reconstruct the

\* Corresponding author. Leibniz Institute for Applied Geophysics, Section S3: Geochronology and Isotope Hydrology, Stilleweg 2, D-30655 Hannover. Tel.: +49 0 511 6432575; fax: +49 0 511 6433665.

E-mail address: [jan-alexander.kunz@liag-hannover.de](mailto:jan-alexander.kunz@liag-hannover.de) (A. Kunz).

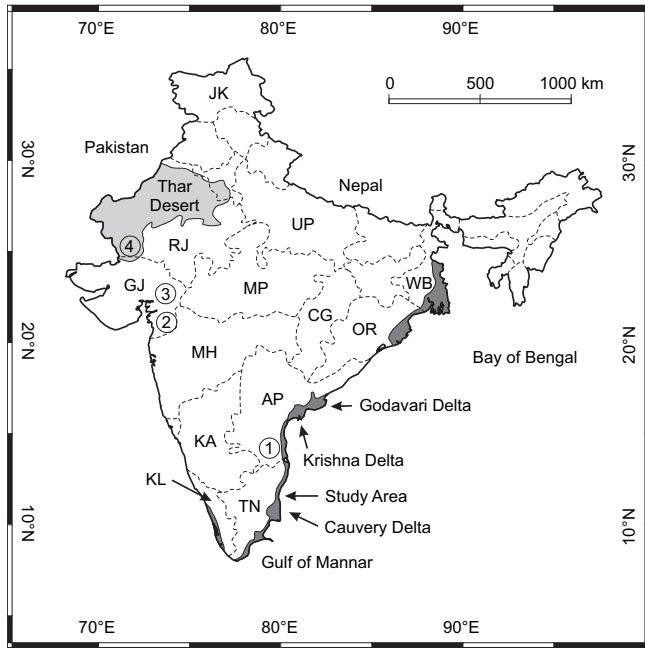


**Fig. 1.** Map showing the distribution of important dune areas in India. The dark grey shaded areas indicate the zones of coastal dunes and sand dunes in the low lying coastal areas. Typical desert sand dunes are only found in the Thar Desert in the north-east of India. AP = Andhra Pradesh, CG = Chhattisgarh, GJ = Gujarat, JK = Jammu and Kashmir, KA = Karnataka, KL = Kerala, MH = Maharashtra, MP = Madhya Pradesh, OR = Orissa, RJ = Rajasthan, TN = Tamil Nadu, UP = Uttar Pradesh, WB = West Bengal. 1 = Pennar River Basin, 2 = Tapi River Basin, 3 = Narmada River Basin, 4 = Luni River Basin.

depositional history of the dunes. The investigation of the dunes in the Cuddalore region gives new insights into periods of sand mobilisation, which are connected to climate conditions, and the age of dune formation. The influence of human activities and the role of sea level changes and tectonic activities as mechanisms for the development of coastal dunes in this place will be discussed briefly.

## 2. Regional setting

The study area (Fig. 2) is located at the Coromandel Coast in Tamil Nadu, approximately 50 km south of Pondicherry. The cities of Cuddalore to the north and Porto Novo to the south are both 20 km away from the area of investigation. The area is characterized by a belt of coastal dunes running parallel to the coast. This dune belt is about 12 km wide in the south near Porto Novo and narrows to the north, until it is less than 5 km wide near Cuddalore. This place was chosen for research because it is sparsely populated. Villages have been built mostly on the dunes. The areas between the dunes are used for agriculture. The accessibility to the dunes in the wide southern part of the dune belt is limited due to the periphery of Porto Novo which is densely populated.

The coastal dunes and sand dunes are separated by slacks and swales and partly stabilized by vegetation. Some of the dunes and adjacent areas are covered by cashew trees. There are also dunes that are still moving and recently constructed houses are buried by large dunes. The height of the dunes varies. Near the coast, they are no more than a few metres high; further inland, the dunes reach heights of more than 10 m. During fieldwork, five dunes at three localities were investigated: one dune situated directly on the coast, two dunes approximately 2 km, and two dunes about 5 km away from the coast. The results of the optically stimulated luminescence (OSL) dating study for both of these latter dunes are presented in

this work. These two dunes are located at the most western position within the dune belt (Fig. 2). Behind this point, no dunes are observed. The dune at sampling position CUD-1 is designated “Temple-Dune” because there is a small Hindu temple nearby. The dune at the sampling position CUD-2 is named “Sherd-Dune” because there is a horizon with plenty of potsherds and bricks.

The Temple-Dune has an altitude of 13 m above sea level and is one of the highest dunes in the study area. A 4-m deep section from top to bottom was excavated, and the layers found have been termed DS1, DS2, DS3a, DS3b and DS5b (Fig. 3). The nomenclature and correlation of the different beds are based on lithology and the geochronological results. The dune body is built up mostly of fine to medium grained sand. The grain size was measured with a Camsizer from samples taken every 10 cm. The sand at the base (DS5b in Fig. 3) is light grey and is more compact than the rest of the dune. This layer contains numerous artefacts including potsherds and fragments from bricks. It is overlain by homogeneous yellowish sand (more than 280 cm thick). In the lower part (DS3b in Fig. 3), this sand is dark-yellow and the higher part (DS3a in Fig. 3) is yellowish grey. This sand shows no sedimentological structures. Separated by an erosional unconformity, an 80 cm thick cross-bedded sand layer occurs (DS2 in Fig. 3). It shows alternating layers of yellowish-grey and brown sand. Each layer is about 10 cm thick and has thin laminae (Fig. 4). The dip angle is about 24° and increases in the higher part. The top of the dune is made up of a 10 cm thick sand layer (DS1 in Fig. 3) with an erosional unconformity at the base. This sand is dark brown and contains many roots.

The Sherd-Dune is located 330 m south of the Temple-Dune. The section is located in an outcrop at the foot of the stoss slope of the dune where sand was excavated. The dune itself is located to the south and is stabilised with large palm trees. Two sections separated by 25 m were studied in detail (Fig. 5). The beds are found are termed DS1, DS2, DS4, DS5a, DS5b, DS5c and DS6 (Fig. 3). The main feature of this dune is a 200 cm thick soil-like bed, which is full of potsherds and fragments of bricks. This bed (DS5a, DS5b and DS5c in Fig. 3) is intercalated into dune sand. Yellow homogeneous sand without artefacts (DS6 in Fig. 3) represents the base of section 1 in the Sherd-Dune. The soil-like bed DS5 continuously overlies the sand. Bed DS5 has a higher content of silt and fine grained sand. It can be subdivided into three parts (Fig. 6). The lowermost part (DS5c in Fig. 3) is grey and shows no layering or bedding. In layer DS5b, dark stratified bands 5–15 mm thick are intercalated (Fig. 6c). At the base they are coarser grained, grading vertically to clay-rich layers. These bands are horizontally stratified with an undulating lower and upper side. The distance between the bands increases in the upper part of bed DS5b. The horizontal extent is limited and the layers are not continuous. In bed DS5a the number of these dark layers decreases. Furthermore, they are thinner, and the distance between them increases. The entire bed DS5 is grey and shows no layering or bedding, except for these intercalated bands. Artefacts are abundant in the entire bed. These are mostly potsherds and remnants of bricks. The bricks are weathered and quite soft, possibly made of clay. Separated with an unconformity, bed DS5 is overlain by dune sand (DS2 in Fig. 3). The base of bed DS2 shows flame structures (Fig. 6b). The sand itself is yellow, non-bedded and does not contain artefacts. Bed DS1 in Fig. 3 represents the uppermost layer. It is more greyish and contains many roots.

In section 2 of the Sherd-Dune, a channel (DS4 in Fig. 3) is incised into bed DS5. The channel is 50 cm wide and 20 cm deep and filled with horizontal laminated sand with layers of dark heavy minerals. On top of the channel deposit and a sharp base, a 5 cm thick sand layer with disturbed bedding occurs (Fig. 7). This layer contains yellow sand alternating with dark layers enriched with heavy minerals. The uppermost part of the dune is built up by 15 cm yellow sand with horizontal bedding. Bed DS5 is

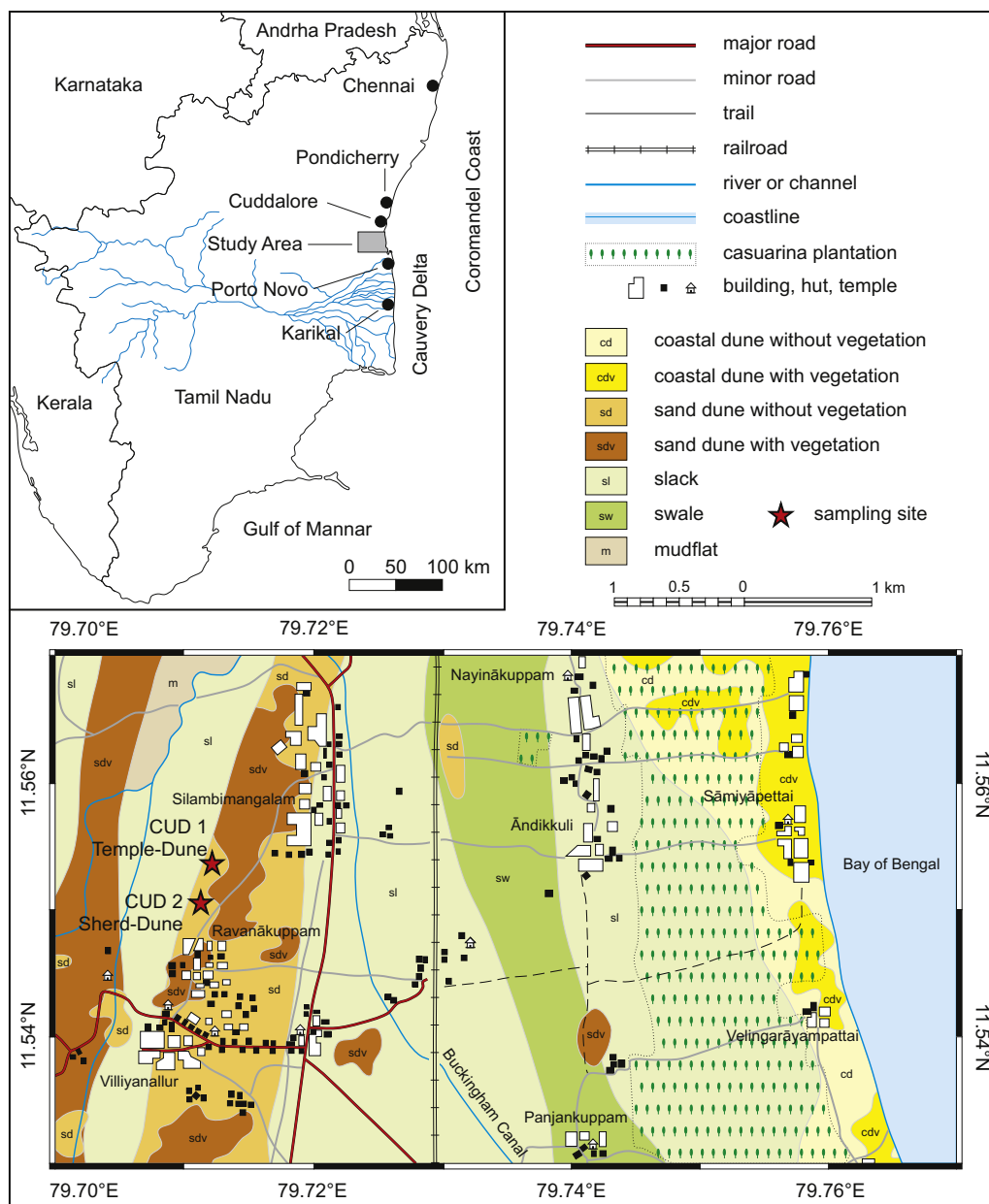


**Fig. 2.** Map showing the study area between Cuddalore and Porto Novo. The sample locations are in the western part of the study area and indicated with a star. CUD 1 is named Temple-Dune due to the close position to a small Hindu temple. CUD 2 is named Sherd-Dune because it contains numerous potsherds. The geomorphology is based on remote sensing using IRS IC-LISS III data and field observations.

characterized by a slightly different colour in the upper part (DS5a) compared with the lower part (DS5b), but has the same sedimentological features and contains numerous artefacts.

From each described bed, samples were taken for OSL dating. The sampling positions are marked in Fig. 3. The correlation of the different beds is described below.

### 3. Materials and methods

#### 3.1. Sample preparation

Samples for optically stimulated luminescence (OSL) dating were collected in opaque plastic tubes hammered into the sediment after cleaning the wall in daylight. The cylinders were sealed to protect the samples from light exposure. Additional material,

approximately 1 kg, was taken for gamma spectrometry. The sample containers were opened under subdued red light in the laboratory. The light exposed outer parts of each sample, about two centimetres on each side, were removed and discarded. The rest of the sample was dried at 50 °C for one or more days depending on the moisture content of the sample. After drying, the samples were sieved and the grain-size fraction between 150–200 µm was taken. Carbonates and organic material were removed by treatment with hydrochloric acid and hydrogen peroxide, respectively. The quartz and potassium-rich feldspar minerals were separated using sodium polytungstate as a heavy density liquid. A detailed description of the sample preparation is given in Aitken (1998) and Ujházy et al. (2003).

The quartz grains (10 g) were subjected to 1 h etching in concentrated hydrofluoric acid, as described in Zander (2000). This

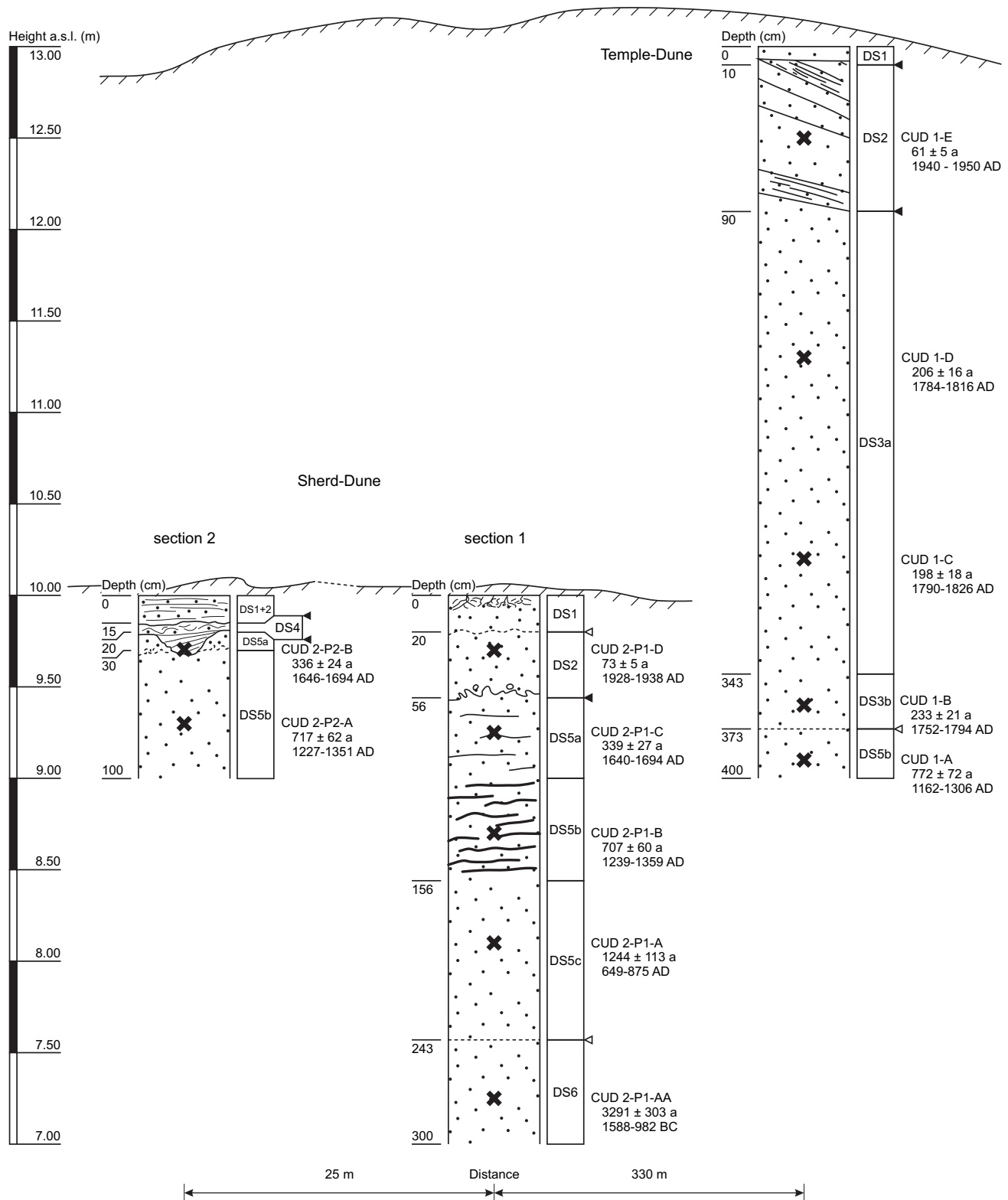


**Fig. 3.** Sections of the Temple-Dune (right) and the Sherd-Dune (middle and left). Both dunes are plotted together to visualise the correlation of the beds. They are not just one morphological form. The lithological description of the beds is given in "2. Regional Setting". The correlation of the beds is based on lithology and geochronology and described in "5.1 Correlation of dunes". The OSL ages are calculated using the Central Age Model. Samples for OSL dating are taken in the year 2006 AD and calculated ages are related to the sampling date. Unconformable boundaries visible in the outcrop are indicated by triangles. Open triangles indicate possible unconformities based on the geochronological results. Artefacts are only intermingled in bed DS5 in all investigated sections. In Figs. 6 and 7 the position of larger artefacts is shown.

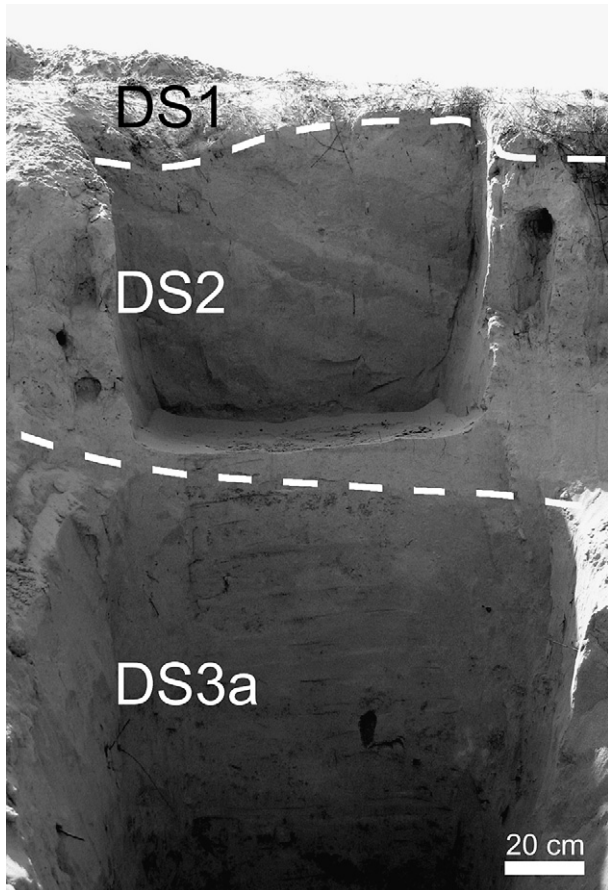


Fig. 4. Upper part of the Temple-Dune showing the beds DS1, DS2 and DS3a.

procedure is necessary to remove remnants of other minerals like feldspars and the outer rim of quartz grains, which is affected by alpha-radiation. The prepared mineral grains were mounted with silicon oil on stainless steel disks with a diameter of 9.8 mm. The IR depletion ratio was used to check feldspar contamination for each sample (Duller, 2003). Some quartz samples had a contamination with feldspar, reflected by an IR depletion ratio  $<0.8$ . These samples were re-etched with hydrofluoric acid and measured again. The second etching removed all feldspar contaminants.

A Risø Reader TL/OSL-DA-15 was used for the measurement of the luminescence signal. The quartz samples were stimulated with blue LEDs with a wavelength of 470 nm and a maximum power of  $40 \text{ mW/cm}^2$ . The emitted light was detected with a bialkali EMI 9235QA photomultiplier tube with a detection window between 200–650 nm. Optical filters are mounted in front of the PM-tube to avoid the detection of the stimulation light. For the measurement of quartz a 7.5-mm thick Hoya U-340 filter with a transmission in the range of 260–380 nm was used. Irradiation of the samples was done by an attached  $^{90}\text{Sr}/^{90}\text{Y}$  beta source with a dose rate of  $0.16 \text{ Gy s}^{-1}$ .

### 3.2. Dosimetry

The natural luminescence signal is mainly the result of the natural radioactivity from radioisotopes of the uranium and thorium chains and  $^{40}\text{K}$  and a minor portion of some other radioisotopes and cosmic radiation. For the age calculation, it is essential to know the dose rate of the sediment, which can be measured by gamma spectrometry with an HPGe (High-Purity Germanium) N-type coaxial detector in the laboratory. For the dosimetry, the infinite matrix approach is assumed (Aitken, 1998). This means for a volume having dimensions greater than the range of radiation, that the rate of energy absorption is equal to the rate of energy emission.

The dose rate was calculated from the activity of  $^{238}\text{U}$ ,  $^{232}\text{Th}$  and  $^{40}\text{K}$  (Aitken, 1998). For the measurement 700 g of the dried sample were homogenised. The material was placed into a Marinelli-beaker and the cap was sealed to avoid loss of  $^{222}\text{Rn}$  in the  $^{238}\text{U}$  decay chain. The beaker was stored for a minimum of four weeks so that the radon disequilibrium could adjust again. Only potassium is measured directly from the decay of  $^{40}\text{K}$  to  $^{40}\text{Ar}$  by release of gamma rays. The activity of  $^{238}\text{U}$  and  $^{232}\text{Th}$  cannot be measured directly by gamma counting because both nuclides have an alpha decay without release of detectable gamma rays. The activity can be calculated from the gamma rays released by the daughter nuclides in the decay chain of  $^{238}\text{U}$  and  $^{232}\text{Th}$ , respectively.  $^{210}\text{Pb}$ ,  $^{214}\text{Pb}$ ,  $^{234}\text{Th}$  and  $^{214}\text{Bi}$  were taken to calculate the activity of  $^{238}\text{U}$  and  $^{212}\text{Pb}$ ,  $^{208}\text{Tl}$  and  $^{228}\text{Ac}$  to calculate the activity of  $^{232}\text{Th}$ . This method allows the monitoring for any radioactive disequilibrium. If there is a radioactive disequilibrium, then the activities for the daughter nuclides from uranium or thorium are not equal. Table 1 shows the results of the gamma spectrometry for the luminescence samples from Cuddalore. For these samples radioactive equilibrium was observed



Fig. 5. Locations of the sections 1 and 2 in the Sherd-Dune. The beds DS1, DS2, DS5a and DS5b are indicated in the middle part.

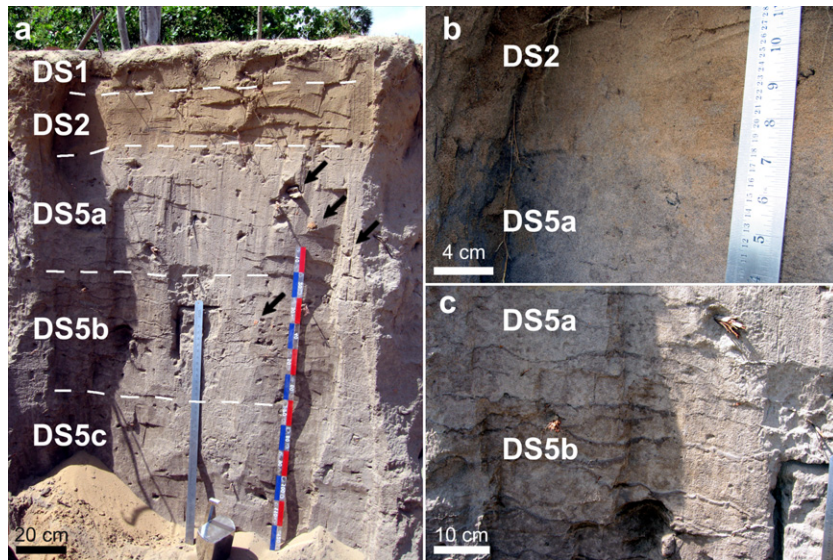


**Fig. 6.** Detailed view of section 1 from the Sherd-Dune. The arrows in figure (a) are indicating larger fragments of bricks and sherds. In (b) the transition between the dune sand in bed DS2 and the soil-like layer DS5a is shown. The flame-structure like boundary indicates that animals or people very likely walked on this surface in the beginning of the sedimentation of bed DS2. In (c) details of the thin clayey and silty bands in bed DS5b are shown. These bands are result of soil forming processes. The transition between DS5a and DS5b is not clear and based on the decreasing amount of clayey bands. In DS5a these bands are thinner, with bigger distances between them and disappearing to the higher part of DS5.

supported by the equivalent activities of the nuclides in the decay chains of  $^{238}\text{U}$  and  $^{232}\text{Th}$ , respectively.

The contribution by alpha particles for dating of quartz grains is negligible due to the etching of the outer rim of the grains. The cosmic radiation, which depends on the latitude, longitude and the thickness of the sediment cover, was calculated by the approach of Prescott and Hutton (1994) and Prescott and Stephan (1982).

### 3.3. Water content

The intensity of the natural radioactivity in the sediment is attenuated by the water in the sediment. This water content has to be estimated and modelled for the duration of burial history. The total annual precipitation in the Cuddalore region is 1236 mm (Indian Meteorological Department, Chennai). Data about the annual variance for the specific region were not available. For Chennai the mean annual precipitation is  $1467 \pm 394$  mm for the period 1991–2004. Due to the near location of the study area to Chennai (Fig. 2) a similar variation could be expected. The seasonal variance of rainfall in this region is much stronger and results in a high variability of water content in the soil during a year. Most of

the precipitation occurs during the NE-monsoon from October to December. During this time 58% (717 mm) of the annual rainfall occurs. Only 30% (374 mm) occurs during the SW-monsoon from June to September. During the winter-season (January and February) and the hot-weather season (March–May) the precipitation decreases so that the total precipitation during this time is about 146 mm.

During sampling in the end of the winter season, the dunes appeared nearly dry. The dunes were not excavated to the ground water table. Constant percolation of water over the year through the dune was assumed. A water content of  $6 \pm 3\%$  for all samples was assumed based on other researches on dunes. Investigations about recharge, infiltration and seasonal variations on soil water content for dunes in Asia have been done by Berndtsson and Chen (1994), Berndtsson et al. (1996) and Dincer et al. (1974). They give values for the water content ranging from  $3 \pm 2\%$  to  $4 \pm 2\%$ . Dunes in North America and Middle America were investigated by Ensign et al. (2006) and Ritsema and Dekker (1994) with a water content ranging from  $5 \pm 5\%$  to  $6 \pm 3\%$ . Lomax et al. (2007) studied dunes in Australia and used a water content of  $3 \pm 3\%$ . The water content of dunes from Europe was investigated by Ballarini et al. (2003), Hilgers et al. (2001), Madsen et al. (2007), and Verhoeven (2002), and ranges from  $5 \pm 4\%$  to  $8 \pm 6\%$ .

For all the different geographic positions and climate zones, the water content in dunes is quite similar. It is mostly around 6%, and we considered this value is as a good estimate of the water content in the dunes here. The error of the water content which represents the seasonal variability ranges between 50% and 100% (depending on the author). In this study an error of 50% was assumed. This represents the variability of the water content between the hot weather season and the monsoon season.

### 3.4. OSL measurement and experimental details

Before starting the measurement with a single aliquot regenerative (SAR) protocol, several tests were performed to check the suitability of the material for OSL dating. In this study the SAR protocol for quartz samples based on Murray and Wintle (2000)



**Fig. 7.** Detail of the event layer DS4 in section 2 of the Sherd-Dune. The arrows indicate bricks and larger potsherds.

**Table 1**

Results of the gamma spectrometry, OSL measurements and the age calculation. The grain size and the water content for all samples is 150–200  $\mu\text{m}$  and  $6 \pm 3\%$ , respectively. Depth in metres (m) is below surface. The dose rate is the sum of the dose rates from the alpha, beta, gamma and cosmic radiation. For the calculation of the total dose rate the conversion factors published by [Adamiec and Aitken \(1998\)](#) were used. A systematic error of 8% is included for the calculation of the dose rate including uncertainties from beta-attenuation, conversion factors, calibration of the gamma detector and effects of past disequilibrium ([Murray and Olley, 2002](#); [Olley et al., 1996](#)). An error of 10% is estimated for the cosmic dose. Ages are calculated using the central age model after [Galbraith et al. \(1999\)](#). The overdispersion ( $\sigma$ ) was calculated from the central age model.

	Sample	depth (m)	K (%)	U (ppm)	Th (ppm)	cosmic dose (mGy a <sup>-1</sup> )	dose rate (mGy a <sup>-1</sup> )	equivalent dose (Gy)	$\sigma$ (%)	Age (a)	
Temple-Dune	CUD 1-E	0.50	1.00 $\pm$ 0.05	0.51 $\pm$ 0.03	7.07 $\pm$ 0.35	0.18 $\pm$ 0.02	1.59 $\pm$ 0.12	0.10 $\pm$ 0.01	21 $\pm$ 3	61 $\pm$ 5	
	CUD 1-D	1.70	1.02 $\pm$ 0.05	0.55 $\pm$ 0.03	8.13 $\pm$ 0.41	0.15 $\pm$ 0.02	1.65 $\pm$ 0.12	0.34 $\pm$ 0.01	6 $\pm$ 1	206 $\pm$ 16	
	CUD 1-C	2.80	1.05 $\pm$ 0.05	0.36 $\pm$ 0.02	4.15 $\pm$ 0.21	0.13 $\pm$ 0.01	1.39 $\pm$ 0.12	0.28 $\pm$ 0.01	11 $\pm$ 2	198 $\pm$ 18	
	CUD 1-B	3.60	1.05 $\pm$ 0.05	0.37 $\pm$ 0.02	4.78 $\pm$ 0.24	0.12 $\pm$ 0.01	1.42 $\pm$ 0.12	0.33 $\pm$ 0.01	15 $\pm$ 2	233 $\pm$ 21	
	CUD 1-A	3.90	1.15 $\pm$ 0.06	0.27 $\pm$ 0.01	2.43 $\pm$ 0.12	0.12 $\pm$ 0.01	1.35 $\pm$ 0.12	1.04 $\pm$ 0.02	10 $\pm$ 2	772 $\pm$ 72	
Sherd-Dune	Section 1	CUD 2 P1-D	0.30	1.00 $\pm$ 0.05	0.95 $\pm$ 0.05	20.12 $\pm$ 1.01	0.19 $\pm$ 0.02	2.42 $\pm$ 0.13	0.18 $\pm$ 0.01	26 $\pm$ 4	73 $\pm$ 5
		CUD 2 P1-C	0.75	1.06 $\pm$ 0.05	0.47 $\pm$ 0.02	6.43 $\pm$ 0.32	0.17 $\pm$ 0.02	1.59 $\pm$ 0.12	0.54 $\pm$ 0.01	10 $\pm$ 1	339 $\pm$ 27
		CUD 2 P1-B	1.30	1.06 $\pm$ 0.05	0.44 $\pm$ 0.02	5.45 $\pm$ 0.27	0.16 $\pm$ 0.02	1.52 $\pm$ 0.12	1.08 $\pm$ 0.03	13 $\pm$ 2	707 $\pm$ 60
		CUD 2 P1-A	1.90	1.04 $\pm$ 0.05	0.38 $\pm$ 0.02	4.15 $\pm$ 0.21	0.15 $\pm$ 0.02	1.40 $\pm$ 0.12	1.75 $\pm$ 0.05	18 $\pm$ 2	1244 $\pm$ 113
	Section 2	CUD 2 P1-AA	2.75	0.98 $\pm$ 0.05	0.37 $\pm$ 0.02	4.54 $\pm$ 0.23	0.13 $\pm$ 0.01	1.35 $\pm$ 0.12	4.46 $\pm$ 0.10	11 $\pm$ 2	3291 $\pm$ 303
		CUD 2 P2-B	0.30	1.02 $\pm$ 0.05	0.64 $\pm$ 0.03	11.1 $\pm$ 0.56	0.19 $\pm$ 0.02	1.87 $\pm$ 0.13	0.63 $\pm$ 0.02	16 $\pm$ 2	336 $\pm$ 24
		CUD 2 P2-A	0.70	1.06 $\pm$ 0.05	0.42 $\pm$ 0.02	4.68 $\pm$ 0.23	0.18 $\pm$ 0.02	1.49 $\pm$ 0.12	1.07 $\pm$ 0.03	13 $\pm$ 2	717 $\pm$ 62

was used. The protocol was modified by inserting a hot-bleach step ([Murray and Wintle, 2003](#)) and the cutheat temperature was chosen equivalent to the preheat temperature ([Wintle and Murray, 2006](#)). Preheat tests, thermal transfer tests and dose recovery tests were performed. The tests were made for the uppermost and lowermost sample of each dune, CUD 1-A and CUD 1-E for the Temple-Dune and CUD 2 P1-AA and CUD P1-D for the Sherd-Dune. Due to the lithological difference of the soil-like bed DS5 in the Sherd-Dune ([Fig. 6](#)), one sample (CUD P1-B) was also used for the same performance tests. The tests were not applied for the samples from section 2 in the Sherd-Dune. The correlation of the beds is obvious and the same luminescence properties of the material are most likely.

Heating of quartz or feldspar can generate movement of charge. The preheat plateau test shows if there is any temperature dependent transfer of charge, which can cause erroneous determination of the equivalent dose  $D_e$  ([Wintle and Murray, 2006](#)). The aliquots of one quartz sample were split into eight groups of three aliquots. Each group was treated with different preheat temperatures. The preheat temperatures are measured in steps of 20 °C from 160 °C to 300 °C. The results of the preheat test are shown in [Fig. 9](#). All samples show no significant increase of the equivalent dose with temperature. The youngest samples CUD 1-E and CUD 2-P1-D showed a plateau over the whole temperature range. The older samples CUD 1-A and CUD 2-P1-B showed a plateau in the range from 160 °C to 240 °C and a slight increase in  $D_e$  for higher preheat temperatures. Only the oldest sample CUD 2-P1-AA shows a plateau in the temperature range from 160 °C to 260 °C and an increase in  $D_e$  for higher preheat temperatures.

Young quartz samples can be affected by the problems of thermal transfer ([Ballarini et al., 2003](#); [Madsen et al., 2005](#); [Wintle and Murray, 2006](#)). This can be checked with the thermal transfer test. The procedure is similar to the preheat test but here the samples are bleached in a Dr. Hönle SOL 2 solar simulator for 2 h. The aliquots were measured in the same way as in the preheat test with increasing temperatures from 160 °C to 300 °C in steps of 20 °C, with thermal transfer implied by a significant increase in  $D_e$  with temperature. We defined a thermal transfer when the  $D_e$  is higher than the error of  $D_e$ . The result of the thermal transfer test is shown in [Fig. 10](#). All samples show the same behaviour in the thermal transfer test. The  $D_e$  is close to zero in the temperature range from 160 °C to 220 °C. For higher preheat temperatures the  $D_e$  value increased, especially for temperatures higher than 280 °C. This indicates that for all samples a preheat temperature lower than 220 °C should be used. Based on preheat and thermal transfer test

in combination with the behaviour of the recycling ratios and the recuperation, a preheat and a cutheat temperature of 160 °C for all samples from the Temple-Dune was chosen. For all samples from the Sherd-Dune, a preheat and a cutheat temperature of 180 °C was chosen.

After determination of the appropriate preheat temperature, dose-recovery tests based on the protocol as described by [Murray and Wintle \(2003\)](#) were carried out. This test determines whether an artificially applied dose can be recovered by the applied SAR protocol. Ten aliquots were bleached in a Dr. Hönle SOL 2 solar simulator for 2 h. The bleached samples were irradiated in the Risø Reader with a fixed beta-dose which is close to the expected equivalent dose. This dose was measured using the SAR protocol applied for the samples. The ratio of the recovered dose to the applied dose should give a value of  $1.0 \pm 0.1$  for a good working SAR protocol. The dose recovery tests showed that for all samples the SAR protocol could recover the given dose. The results of the dose recovery test are summarized in [Table 2](#). Based on the results of the performance tests a SAR protocol ([Table 3](#)) was developed and the  $D_e$  values of the samples were measured with this protocol.

### 3.5. Age calculation

The OSL-ages are calculated by dividing the equivalent dose ( $D_e$ ) by the dose rate of the sediment including the contribution of the cosmic rays and the attenuation by the water content. For the calculation of the equivalent dose different age models are available. The decision for an appropriate model depends on the distribution of the  $D_e$  values from the SAR-measurement. [Arnold et al. \(2007\)](#) and [Bailey and Arnold \(2006\)](#) provided a decision making process between central age model (CAM) and minimum age model with three components (MAM-3). Both models are described in [Galbraith et al. \(1999\)](#). The dose distribution of the equivalent doses for the samples from the Temple-Dune and the

**Table 2**

Results for the dose recovery test. Ratio gives the ratio between the applied dose and the measured dose.

Sample	Applied dose	Ratio	Recycling ratio	Recuperation
CUD 1-A	1 Gy	0.95 $\pm$ 0.04	1.00 $\pm$ 0.03	<1%
CUD 1-E	1 Gy	0.93 $\pm$ 0.03	1.01 $\pm$ 0.03	<1%
CUD 2-P1-AA	5 Gy	0.95 $\pm$ 0.02	0.99 $\pm$ 0.02	<1%
CUD 2 P1-B	1 Gy	0.96 $\pm$ 0.04	1.02 $\pm$ 0.02	<1%
CUD 2 P1-D	0.5 Gy	0.95 $\pm$ 0.03	1.01 $\pm$ 0.04	<2%

**Table 3**  
Single aliquot regenerative (SAR) protocol used for the measurement of the samples.

Step	Treatment	Observed
1	Give regenerative dose $D_i$ (0.16–6.57 Gy)	
2	Preheat 160 °C for 10 s for samples from the Temple-Dune Preheat 180 °C for 10 s for samples from the Sherd-Dune 5 °C/s heating rate for samples from both dunes	
3	OSL with blue LED 40 s @ 125 °C	$L_i$
4	Give test dose $D_t = 0.82$ Gy	
5	Cutheat 160 °C for 0 s for samples from the Temple-Dune Cutheat 180 °C for 0 s for samples from the Sherd-Dune 5 °C/s heating rate for samples from both dunes	
6	OSL with blue LED 40 s @ 125 °C	$T_i$
7	OSL with blue LED 40 s @ 290 °C	

For the natural sample  $i = 0$  and  $D_0 = 0$ . The whole sequence is repeated for several regenerative doses, including a zero dose and a repeat dose. Regenerative doses  $D_i$  depending on the expected age of the sample. Preheat tests give a first possible age. Doses are chosen in that way, that they bracket the natural dose. In this table the range of all given doses for all samples is given. The ratio between  $L_i/T_i$  is used for the calculation of the equivalent dose. The OSL signal from step 7 (hotbleach) is not used.

Sherd-Dune was analysed using the Kolmogorov–Smirnov (K–S)-Test, and all the distributions were appeared to be normal (Fig. 8). The distribution of Sample CUD 2 P1-A is slightly skewed. The K–S test for this sample gives a P value of 0.149 which is below the significance level of 0.196. This suggests that it is close to the threshold to a non-normal distribution but still regarded as a normal distribution.

Bailey and Arnold (2006) recommend the use of the CAM for well-bleached sediments, such as aeolian sediments, and when the overdispersion ( $\sigma$ ) is smaller than 50%. Based on these suggestions, the central age model from Galbraith et al. (1999) was used for all samples. The overdispersion values are listed in Table 1.

#### 4. Results

Altogether, 12 samples for OSL dating were measured and the ages were calculated. The results of the dosimetry, the OSL measurement and the age calculation are summarized in Table 1 and Fig. 3.

The annual dose rates for the samples from the Temple-Dune range from  $1.35 \pm 0.12$  mGy  $a^{-1}$  to  $1.65 \pm 0.12$  mGy  $a^{-1}$  and for the samples from the Sherd-Dune from  $1.35 \pm 0.12$  mGy  $a^{-1}$  to  $2.42 \pm 0.13$  mGy  $a^{-1}$  (Table 1). The dose rates for the topmost and hence younger samples are higher than the older samples from the lower beds. The dose rate of sample CUD 2 P1-D has a value of  $2.42 \pm 0.13$  mGy  $a^{-1}$  clearly higher than the other samples. The higher uranium and thorium content in this bed (DS2 in section 1 in the Sherd-Dune) are the reason for the significant higher dose rate. This is most likely related to the higher content of heavy minerals. Along the south east coast of Tamil Nadu, many places with higher concentrations of heavy minerals are known (Chandrasekharan and Murugan, 2001; Mohan and Rajamanickam, 2000). The dose rate of the sediment is strongly dependent on the minerals and their concentrations of uranium, thorium and potassium. Comparing the dose rates used for luminescence dating of dunes from other places in the world, the values for the annual dose rate range from around 0.2 mGy  $a^{-1}$  for dunes in New Mexico (Kocurek et al., 2007) up to values around 3.6 mGy  $a^{-1}$  for dunes in China (Li et al., 2002). Extremely low values of the dose rate are normally found in quartz-rich sediments such as coastal dunes (Berger et al., 2003) or dunes in geologically old areas such as southern Africa (Chase and Thomas, 2007) or Australia (Lomax et al., 2007). The dose rates obtained here are in the typical range of quartz-rich dune sands.

The equivalent doses ( $D_e$ ) measured with OSL on quartz for the samples from the Temple-Dune range from  $0.10 \pm 0.01$  Gy to  $1.04 \pm 0.02$  Gy (Table 1). The calculated ages are between from  $61 \pm 5$  years (CUD 1-E) and  $772 \pm 72$  years (CUD 1-A). There is an increase of  $D_e$  and of age with depth. Sample CUD 1-C has a slightly lower  $D_e$  and lower age than the samples from above and below (Fig. 3). The 1-sigma standard deviation makes an equal deposition age likely for CUD 1-C and CUD 1-D. Based on the geochronology three periods of increased sand mobility can be identified in the Temple-Dune. The first depositional period took place at  $772 \pm 72$  years, a second period around 210 years ago and a quite recent period at  $61 \pm 5$  years before today (Fig. 3).

In section 1 from the Sherd-Dune, the obtained  $D_e$  range from  $0.18 \pm 0.01$  Gy to  $4.46 \pm 0.01$  Gy (Table 1). The calculated ages are ranging from  $73 \pm 5$  years (CUD 2 P1-D) to  $3291 \pm 303$  years (CUD 2 P1-AA). There is an increase of  $D_e$  and of age with depth (Fig. 3). The dating results for the Sherd-Dune indicate at least three periods of sand mobility and one event. The oldest deposition occurred  $3291 \pm 303$  years ago, followed by a longer period of sedimentation from  $1244 \pm 113$  years to  $339 \pm 27$  years ago. This was discontinued by a fluvial event at  $336 \pm 24$  years ago (visible in section 2). The third period of sand accumulation took place  $73 \pm 5$  years ago.

#### 5. Discussion

##### 5.1. Correlation of dunes

The correlation of the Temple-Dune and the two sections from the Sherd-Dune is based on the lithology and geochronology. In Fig. 3, the different beds are indicated by capital letters in the right column beside the lithological section.

The uppermost part of the Temple-Dune and Sherd-Dune is assigned as bed DS1, a weakly and most recently developed soil. The uppermost position in the dunes represents recent deposition of sand and modern soil formation. In section 2 of the Sherd-Dune, the uppermost layer belongs either to DS1 or to DS2. This bed was designated DS1 + 2, because it is not possible to correlate it with DS1 or DS2 from section 1. In the outcrop, the uppermost beds of the two sections correlate to each other (Fig. 5). However, in section 2 the differentiation into DS1 and DS2 is not clearly visible. A recent deposition within the last 10 or 20 years is likely.

Bed DS2 in the Temple-Dune section and the Sherd-Dune section has a similar depositional age of around 65 years before today. In the Sherd-Dune, bed DS2 does not show the cross-bedding which is characteristic of the Temple-Dune and the altitude of both horizons is also different. However, based on the time of deposition and the unconformity at the base in both dunes, these horizons formed synchronously and hence can be correlated.

Bed DS3 is only present in the Temple-Dune section. The subdivision into DS3a and DS3b is based on the different colours of the sand: DS3b is dark yellow and DS3a more greyish. The sand gives a depositional age of around 210 years. At the sections 1 and 2 of the Sherd-Dune, deposits with this age were not found. The outcrop is located at the lower part of the dune slope.

Bed DS4 occurs only in section 2 of the Sherd-Dune section and represents an event with fluvial activity (Fig. 7). The filling of the channel and the disturbed upper layer are attributed to bed DS4.

Bed DS5 is subdivided into three parts DS5a, DS5b and DS5c based on sedimentological features (Fig. 6) and OSL ages. This layer is present in all dunes. It is also visible in the field and acts as a marker horizon based on its relatively large spatial extension. DS5a is characterized by a depositional age of around 350 years, and has few thin clayey bands intercalated. The sedimentological features of bed DS5a are slightly different in section 1 and 2 (Fig. 7). In section 2 it is brownish grey and the clayey bands are not

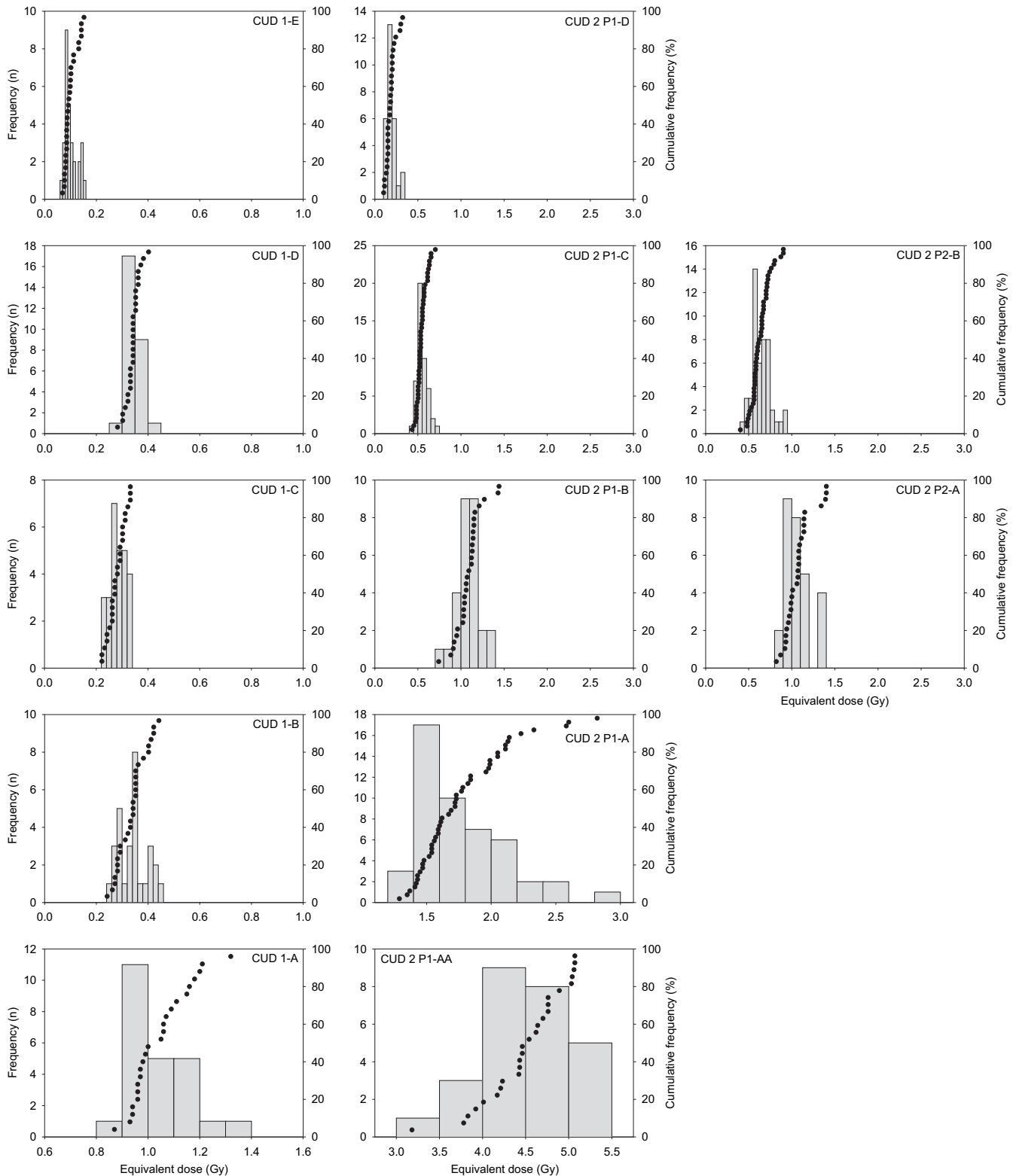
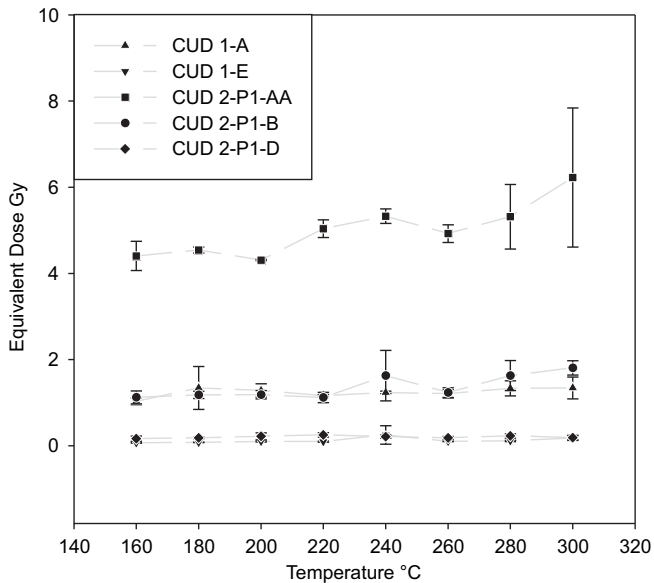


Fig. 8. Dose distributions of the investigated samples.

present. This layer is attributed to DS5a because it is also characterized by greyish sand, which is indicative of bed DS5 and it is older than the filling of the channel dated to approximately 300 years and younger than DS5b with an age of about 700 years. The transitional border to DS5b could also be slightly lower in that

profile. Bed DS5b is characterised by numerous dark clayey bands (Fig. 6c). They are thicker than in DS5a. The depositional age of DS5b is about 700 years. This bed occurs in all dunes, although the intercalated clayey bands occur only in section 1 of the Sherd-Dune section. In the Temple-Dune section the lowermost part is



**Fig. 9.** Results of the preheat plateau test for samples from the Temple-Dune (CUD 1-A and CUD 1-E) and the Sherd-Dune (CUD 2-P1-B, CUD 2-P1-D, and CUD 2-P1-AA). For each temperature the mean of three aliquots and the standard deviation is shown. For a detailed description see “3.4 OSL Measurements and Experimental Details”.

attributed to DS5b based on the OSL age. Bed DS5c is only visible in section 1 of the Sherd-Dune. It shows no intercalated clayey bands, and the OSL age of  $1244 \pm 113$  years is older than in the higher beds.

The base of the section 1 from the Sherd-Dune is made by bed DS6. This is yellowish sand without any artefacts and has an OSL age of  $3291 \pm 303$  years. The lithology and geochronology is clearly different from bed DS5, and hence it is considered as a distinct layer.

## 5.2. Discussion of results and interpretation

The sedimentological successions in the dunes show unconformities, changes in the direction of bedding, erosional features,

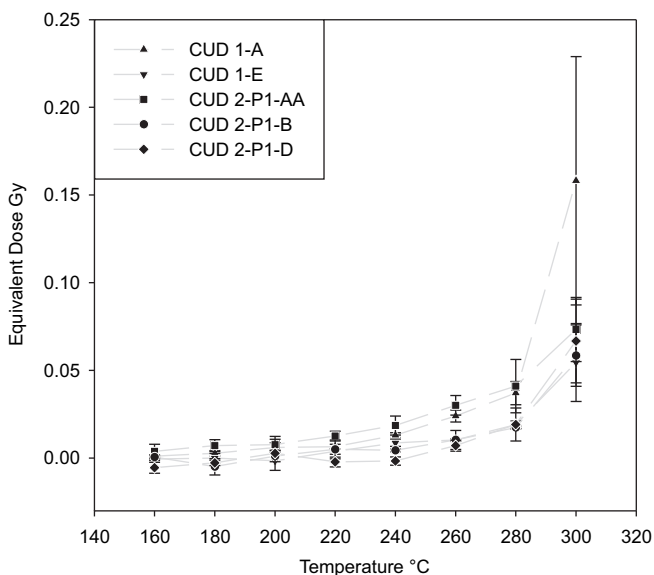


**Fig. 10.** Results of the dose recovery test for samples from the Temple-Dune (CUD 1-A and CUD 1-E) and the Sherd-Dune (CUD 2-P1-B, CUD 2-P1-D, and CUD 2-P1-AA). Thermal transfer can be observed for all samples at preheat temperatures higher than 260 °C. For each temperature the mean of three aliquots and the standard deviation is shown.

water escape structures and remnants of human settlement. These features reflect changes in the environmental conditions. Dunes are sediment archives which can reflect environmental and climate changes. They can be used to reconstruct periods of aridity and humidity connected with climatic changes. In several studies, dunes were used to reconstruct the climate and environmental conditions in many regions of the world. Intensive research was done on dunes in Australia, southern Africa and North America. The basic concept in interpreting the dunes is that periods of sand accumulations are related to drier climatic conditions and unconformities as well as palaeosols are related to humid conditions with a stabilisation of the land surface. This was successfully applied to dunes in Australia for example by Fitzsimmons et al. (2007), Lomax et al. (2003), and Twidale et al. (2007). In southern Africa, more recent studies on dunes were carried out by Chase and Thomas (2007), Holmes et al. (2008), and O'Connor and Thomas (1999). They found that dune development is not generally related to arid climatic conditions. The supply or availability of sediment and the wind strength are important factors. The sediment supply is controlled by vegetation cover, fluvial activities or lake level fluctuations. In coastal areas, the sediment supply and hence the dune development is related to sea level changes (Murray-Wallace et al., 2002; Radies et al., 2004). During low stands, more sand is available. Another important factor for dune development is human impact, especially for young dunes. The vegetation cover can be disturbed or destroyed by human activities which can lead to remobilisation of dunes (Hesse et al., 2004; Sun, 2000; Wolfe et al., 2001). A summary about dunes as palaeoclimate proxies is given by Lancaster (2008). Cautionary critiques for using dunes as palaeoclimate proxies are given by Munyikwa (2005) and Telfer and Thomas (2007).

The results of this study show different periods of sand movement and stabilisation of the land surface. However, the interpretation of the dune development in this area is complex. The climate conditions are mainly forced by the monsoon. Changes in the monsoon activity could be reflected in sand accumulation during drier periods. A second important point is sea level change during the Quaternary, as indicated by the geomorphology of the dune belt. The dune ridges are parallel to the present coast. The younger parts of the dunes are often influenced by human activities.

### 5.2.1. Climate and human impact

The climate in the study area is influenced by the monsoon. In contrast to the whole subcontinent, the amount of annual rainfall in Tamil Nadu is dominated by the NE-monsoon, due to its location on the lee side of the Western Ghats Mountains. Therefore, the NE-monsoon rains are an important factor for the ecological and geomorphological evolution of that region. Although the SW-monsoon brings only low amounts of rainfall, it still has influence in that region (Gregory, 1989; Mooley and Parthasarathy, 1983). Fluctuations in the NE-monsoon intensity have been investigated, e.g., by Dhar et al. (1982) and Walsh et al. (1999); the SW-monsoon intensity by Kale et al. (2004) and Mooley and Parthasarathy (1984). Monsoon activity in India using sediment archives was investigated by Kale (1999), Kale et al. (2000, 2004), Nigam and Khare (1994), Prasad and Enzel (2006), and Thomas et al. (2007). Kale (1999) compared the drainage data of Indian rivers for the last 150 years with the precipitation record in India. There is a direct correlation between higher monsoon activity and increased drainage and flood events. This concept was applied for palaeofloods of the Luni River in the Thar Desert by Kale et al. (2000). For the Penner River basin in south India, Thomas et al. (2007) used the same concept to establish a history of the monsoon activity for south India. In the study of Prasad and Enzel (2006), a connection between decreased dune mobilisation during increased monsoon activity is observed.

They assume a stabilisation of the land surface through vegetation because of wetter climate conditions in periods of increased monsoon activity. Liu et al. (1998) and Thompson et al. (2000) investigated the monsoon activity for southern Asia using pollen records, dust records and geochemical proxies from Himalayan ice cores. The results of these studies are summarized and compared with our study in Fig. 11. The results of the present study correlate with the periods of dry and wet climate conditions in India.

Due to the intensity of the NE- and SW-monsoon, it is difficult to compare the dunes with records from other parts of India. Extreme SW-monsoon events have also strong impacts in Tamil Nadu, especially the northern part of Tamil Nadu, where the study area is located. Floods and droughts in connection with the SW-monsoon were studied by Mooley and Parthasarathy (1983). In 1961, India was affected by very strong rainfall. The highest amount was in western Rajasthan and Saurashtra and in the northern parts of Tamil Nadu as well as in the south-east of Andhra Pradesh (Fig. 1). A similar precipitation pattern occurred in 1899, when rainfall was much lesser than the mean causing droughts in these states. Strong changes in SW-monsoon and climate changes on a larger scale could have also influenced the rainfall in the study area in the past.

The dune sand in bed DS6 of the Sherd-Dune section (Fig. 3) could represent a period of drier climate conditions caused by weaker monsoon activity. The time of deposition,  $3291 \pm 303$  years before present, correlates with the so-called 3.5 ka event (Fig. 11). This event at 3.5 ka BP (Kale et al., 2004) marks the minimum of monsoon precipitation during the mid-Holocene and hence correlates to a period of increasing aridity. This trend of weakening monsoon and increasing aridity can be observed through the whole mid-Holocene in south Asia (Kale et al., 2004). From that time, the climatic conditions changed to warm and dry conditions with interruptions of increased monsoon activity.

Bed DS5 apparently seems to accumulate continuously from the dune sand in bed DS6 (Fig. 3). However, the OSL-ages indicate a hiatus. DS5 differs strongly from the other layers. It is grey and shows no bedding or other sediment structures. The layer is full of potsherds and fragments of bricks, indicating human activity and settlement in this region. The foundation of the settlement was very likely between  $3291 \pm 303$  years and  $1244 \pm 133$  years before present (1588 BC–875 AD), and lasted until approximately  $339 \pm 27$  years before present (1640–1694 AD). Compared to other archaeological sites in Tamil Nadu, evidence for early settlement is found in Kampanmedu where bricks are dated to an age of 400 AD and in Arikamedu where pottery with an age of 300 BC was found (Ramaswamy and Duraiswamy, 1990). Both places are around 80 km south of the study area. Arikamedu is an ancient port, which

existed since around 200 BC and is famous for the trade with the Romans (Begley, 1996). The bed DS5 seems to reflect sand mobilisation due to human impact and a change to more humid climatic conditions indicated by features from soil forming processes. Bed DS5 was deposited during a period which is described by Kale et al. (2004) and Thomas et al. (2007) as a period of increased monsoon activity in India with a maximum rainfall lasting from 750 to 500 years before present (Fig. 11). This period could be reflected in bed DS5b with a depositional age of  $707 \pm 60$  years before present.

The thin clayey-silt bands (Fig. 6c) are derived from illuvation processes. Finer grained material is transported through the sandy horizon. This is part of a soil forming process and can be observed in many dunes. The A-horizon from the originally developed soil above these layers is missing here. It is very likely eroded. The better climate conditions could have also supported the foundation of settlements and agricultural activities in this region. During humid periods, stabilisation of the land surface and formation of soils would be expected. The sedimentation of sand is reduced or stopped, as observed for dunes in Australia by Fitzsimmons et al. (2007) and Lomax et al. (2003). The settlement activities in the study area could have partly disturbed or removed the vegetation cover resulting in reactivation of local dunes. Hesse et al. (2004) mentioned that the vegetation cover controls the dune development stronger than wind strength. The influence of human impact on dune remobilisation is described by Sun (2000), Sun et al. (2006) and Wolfe et al. (2001). The combination of periods with stabilised land surface and periods with active dunes would explain the more or less continuous growth of this horizon for a longer time. The discontinuous and localized development of the bed DS5 is also supported by the fact that the clay bands in section 2 are missing. The OSL-ages are slightly different at the same elevation, indicating paleorelief. The phenomenon of stabilised dunes and active dunes can be observed in this area today. Due to house building activities or agriculture, the vegetation cover is removed and dunes are activated. During fieldwork, recently constructed houses partly covered by dunes were observed.

The sedimentological features of bed DS4 (Fig. 7) in section 2 of the Sherd-Dune section (Fig. 3) give evidence for a fluvial event. The filling of the channel yielded an OSL age of  $336 \pm 24$  years, showing a deposition between 1646 and 1694 AD. The 5 cm thick disturbed layer on top of the channel filling shows water escape structures. There are different mechanisms responsible for soft-sediment deformation: liquefaction or fluidization, reverse density gradation, slumping or slope failure and shear stress (Mills, 1983; Owen, 2003). In this case, the structures in bed DS4 are related to liquefaction or fluidization. The development of these structures is

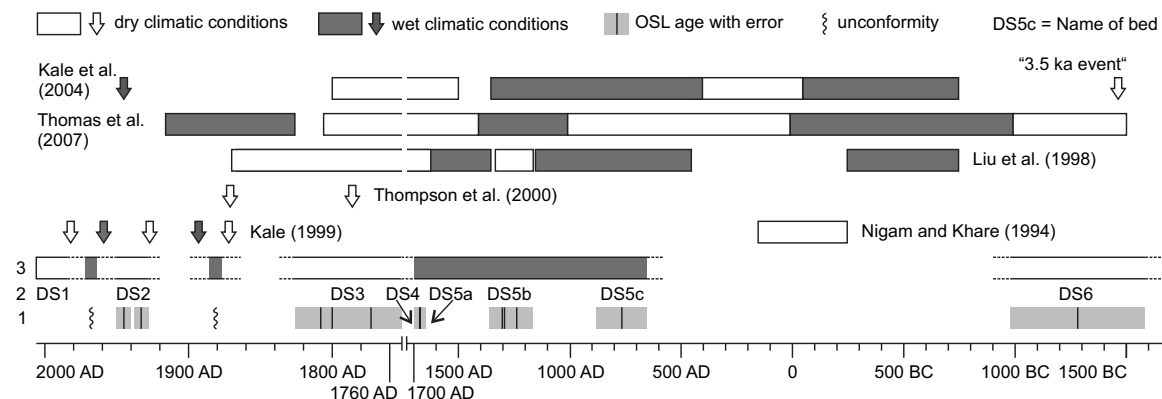


Fig. 11. Comparison of the results of this study with other studies about the monsoon history in India. 1 = OSL ages with errors. 2 = Names of beds according to OSL samples. 3 = Monsoon history for the study area based on these results and interpretation. Arrows indicate short climatic events. NB: Change of scale between 1760 AD and 1700 AD.

a function of rapid dewatering of saturated fluid-supported sediments (Mills, 1983). The triggering mechanism can be overloading and sediment gravity flow (Neuwerth et al., 2006), earthquakes, storms or rapid deposition in flood events (Mills, 1983). The latter is the most likely reason for the development of the soft-sediment deformation structures in bed DS4. A flood event is also supported by the channel at the bottom of bed DS4. The source for the flood could be the river which is approximately 600 m in the west of the sampling location (Fig. 2). In the Temple-Dune section and in section 1 of the Sherd-Dune, sediments with signs of a flood event are not present. There are unconformities between beds DS5b and DS2 in the Sherd-Dune section (Fig. 6b) and beds DS5b and DS3b in the Temple-Dune section (Fig. 3) indicating periods of non-deposition.

Based on the work of Lomax et al. (2003) and Tchakerian and Lancaster (2002), this can be related to more humid conditions which do not support the accumulation of dunes. It is not clear whether this event is related to a general increase of rainfall in India or it is a single event. Historic records are not available for that time period. The oldest record is from the year 1732 AD (Walsh et al., 1999). This event occurred at the end of a period with higher monsoon activity and at the beginning of Little Ice Age. Compared to the work of Kale et al. (2000, 2004) and Thomas et al. (2007) the duration of this period shows regional differences. The flood history of the Luni River in the Thar Desert (northwest India) shows a maximum rainfall in the time between 750 and 400 years BP (Kale et al., 2000). In the Pennar River basin in south-east India (Fig. 1), a period of high monsoon activity lasting from 1000 to 600 years BP is represented by flood events (Thomas et al., 2007). In the Narmada and Tapti river basins in western central India (Fig. 1), the flood record shows a stronger monsoon activity between 1700 and 500 years BP (Kale, 1999). Another possible interpretation of this unconformity is aeolian deflation during arid periods in the beginning of the Little Ice Age. Deposits of this event are found in bed DS3.

The accumulation of the 2.8-m thick dune sand in bed DS3 in the Temple-Dune section (Fig. 3) occurred very quickly. The OSL ages from the samples taken from this horizon reflect deposition between  $233 \pm 21$  years and  $198 \pm 18$  years before present (1752–1826 AD). The deposition of this dune sand coincides with the Little Ice Age (16th century to the mid 19th century). The Little Ice Age in India is reflected by a reduction of great floods between 1500 and late 1800s AD (Kale et al., 2004) and great droughts during 1790–1796 AD and 1876–1877 AD (Mooley and Parthasarathy, 1983; Thompson et al., 2000). The droughts were initiated by failure of the monsoon. During those times of reduced precipitation, sand was reactivated and rapid deposition of large dune sands was possible. During the Little Ice Age, the sea level at the east coast of India was 1 m below the present low tide level (Banerjee, 2000). The regression made more sand available. Sediments with the same age as in the Temple-Dune section are not found in the Sherd-Dune section. The reason is that the outcrop is located at the margin of the dune slope. In the core of the dune, sand deposited during the Little Ice Age could be expected.

The hiatus between bed DS3a and DS2 visible in the Temple-Dune section (Figs. 3 and 4) indicates a period of wet climate conditions due to increased precipitation and stabilisation of the land surface by vegetation (Hesse et al., 2004; Tchakerian and Lancaster, 2002). This unconformity developed between approximately 200 years and 60 years before present. For this time period, an increase in rainfall across India is reported by Kale (1999) and Walsh et al. (1999).

Bed DS2 in the Temple-Dune and Sherd-Dune sections (Fig. 3) indicates a period of sand movement. The reason could be a reduced precipitation in combination with reduced vegetation

cover and human activities. The depositional age of the sand in bed DS2 in the Temple-Dune with  $61 \pm 5$  years and  $73 \pm 5$  years in the Sherd-Dune falls into a period of reduced rainfall in India. Kale (1999) reports a minimum in the all-India monsoon rainfall in the years from 1920 AD to 1945 AD (Fig. 11). This minimum was also observed by Dhar et al. (1982) for the NE-monsoon. The sedimentation of the dune sands in bed DS2 ends abrupt with an unconformity, which is clearly visible in the Temple-Dune (Fig. 4). In the Sherd-Dune this unconformity is weakly developed (Fig. 6). Since 1945 AD, monsoon activity has increased with a maximum in 1964 AD (Kale, 1999; Mooley and Parthasarathy, 1983). This high precipitation could be the reason for the stabilisation of the land surface by vegetation. Bed DS1 indicates again a period of sand movement. This is most likely induced by human activities. The influence of human activities plays an important role here. However, that the periods of sand movement and unconformities coincide with changes in the precipitation.

### 5.2.2. Sea level change

The development of dunes in coastal areas is often connected to changes in sea level. During low stands the availability of sediment is higher and coastal dunes develop more frequently. Different generations of dunes can reflect the different sea level stands and also reflect the palaeocoastline in this specific area (Murray-Wallice et al., 2002). The dune belt between Porto Novo and Cuddalore runs parallel to the present coastline. It is likely that sea level changes are playing a role in the development of this dune belt. From the available data, it is difficult to find a direct relation between dune development and sea level change in this area, as the base of the dunes was not reached during fieldwork.

The global sea level increased during the Holocene. The marine transgression is not continuous and interrupted by phases of regressions, e.g., during the Little Ice Age (Siddall et al., 2007). In India the sea level at the south east coast reached a maximum of +4 m above the present low tide level (LTL) around 4 ka, indicated by marine terraces (Banerjee, 2000). It remained stable until around 2 ka (Achyuthan and Baker, 2002; Banerjee, 2000; Brückner, 1988). From that time the sea level is falling. During the Little Ice Age it reached a minimum of –1 m below present LTL (Banerjee, 2000). After the Little Ice Age the sea level reached the present level.

During the Holocene sea level high stand the coastline was approximately 1 km inland, which could be the reason for the development of coastal dunes at this place. The sand of bed DS6 yielded an age of deposition at  $3291 \pm 303$  years and very likely correlates to the Holocene sea level high stand. The sea level low-stand during the Little Ice Age could be reflected in bed DS3 with a deposition age between  $233 \pm 21$  and  $198 \pm 18$  years. The sand accumulated quite fast indicating a greater availability of sand. The drier climate with reduced vegetation cover could enhance the movement of sand.

It is difficult to use this data here for sea level reconstruction because the area is tectonically unstable. The evolution of the Cauvery Delta south of the study area indicates neotectonic activities during the Holocene (Ramasamy, 2006). The delta itself is controlled by NE–SW and ENE–WSW lineaments which have been active since the Late Cretaceous. In the south of the Cauvery Delta the Mio-Pliocene sandstone formation has been uplifted for the past 6.1 ka (Ramasamy et al., 2006). Due to this uplift, the main course of the Cauvery River shifted from south to north after 2.5 ka. Between Pondicherry and the northern part of the Cauvery Delta a NE–SW striking graben structure developed in the Holocene. The subsidence of this graben is also indicated by the changing flow direction of the rivers from north to south in the Pondicherry area (Ramasamy, 2006). Neotectonic activities in this area are also

shown by earthquakes with magnitudes up to  $M \sim 5.6$  in the year 2001 (Raval, 2002). The subsidence rate of the area between Porto Novo and Pondicherry is not known. If the subsidence rate is slower than sea level regression the dunes reflect possible palaeobeach lines. If the rate is higher, the coast will show a transgression. More work is required to find more arguments for a relation between sea level and the dune evolution in this area.

## 6. Conclusion

This study presents the first results of OSL dating of two dunes located at the western part of a dune belt running parallel to the coast of south east India between Pondicherry and Karikal (Fig. 2). The OSL investigation shows that the material in south-east India is suitable for this method. The sedimentology and the geochronology of the dunes show periods of sand accumulation and stabilisation of the land surface in the last 3500 years in southeast India. The interpretation of dune development in this area is complex. There are different factors, including climatic changes due to changes in monsoon activity, sea level changes which could be responsible for the development of the whole dune system, and human impact especially for the younger parts of the dunes. Based on the geochronological and sedimentological investigations, an interpretation of the deposition history of the dunes is presented.

The dune sand in bed DS6 in section 1 of the Sherd-Dune (Fig. 3) represents a period of drier climatic conditions caused by a weakening of the monsoon activity  $3291 \pm 303$  years before present (1588–982 BC). Climate changed during the Late Holocene to wetter conditions due to an increasing monsoon activity (Fig. 11).

The bed DS5 differs strongly from the other layers in the dunes. The high amount of potsherds and brick fragments, the grey colour and the absence of sedimentological structures indicates a period of settlement and stabilisation of the land surface. Settlement activities at the studied sites started between  $3291 \pm 303$  years and  $1244 \pm 113$  years before present (1588 BC–875 AD) and ended possibly  $339 \pm 27$  years before present (1640–1694 AD). The deposition took place during a period which is described as having increased monsoon activity in India by Kale et al. (2004) and Thomas et al. (2007). The clayey-silty bands in section 2 of the Sherd-Dune are from soil forming processes and support the assumption of a wetter climate.

Bed DS4 in section 2 of the Sherd-Dune (Fig. 7) shows a flood event at  $336 \pm 24$  years before present (1646–1694 AD). The Temple-Dune and the Sherd-Dune sections show distinct erosional unconformities between the beds DS5b and DS3b as well as DS5a and DS2, respectively. This unconformity represents a period of non-deposition. Lomax et al. (2003) and Tchakerian and Lancaster (2002) suggested that surface stability could be related to wet climate conditions which do not support sand mobility. The results are evidence for an extended period of increased monsoon activity. This interpretation is in contrast to the work of Kale et al. (2000, 2004) and Thomas et al. (2007), who proposed increased monsoon activity until 600 years before present. This interpretation could be related to regional differences in climate conditions. Alternatively the unconformity could be due to aeolian deflation during an arid period at the beginning of the Little Ice Age.

The 2.8-m thick deposit of dune sand represented by bed DS3 in the Temple-Dune section shows a period of dry climate conditions generated by a weakening of the monsoon. The time of deposition falls into the period dated  $233 \pm 21$  years and  $198 \pm 18$  years before present (1752–1826 AD) of the Little Ice Age (Fig. 11). This period is characterised by dry climate and droughts in India due to the failure of the monsoon (Thompson et al., 2000). During the Little Ice Age, the sea level in south east India was  $-1$  m lower than the present LTL (Banerjee, 2000) resulting in an increased availability of sand.

The deposits of bed DS2 in the Sherd-Dune and the Temple-Dune sections indicate a period of sand mobility, most likely due to less precipitation in combination with a decrease in vegetation cover and human activities. A more recent general decrease of the precipitation in India was observed for the time period between 1929 and 1948 AD (Fig. 11) (Kale, 1999). This minimum is also described by Dhar et al. (1982) for the NE-monsoon. The hiatus between the beds DS3a and DS2 and the beds DS2 and DS1 correlate with periods of increased precipitation (Kale, 1999). Great flood events during this time, related to an increased monsoon activity in India, are reported by Kale (1999) and Thomas et al. (2007). During these periods, the land surface was stabilised by vegetation which made the accumulation of sand unlikely. The impact of human activities on the remobilisation of sand is especially for the younger parts of the dune important. The possibility that dune activity is triggered by human activities cannot be excluded. However, the sand accumulation and unconformities coincide with the fluctuations in the precipitation rate of this region.

The geomorphology of the dune system between Porto Novo and Cuddalore make it obvious that the dune ridges are related to sea level changes, but subsidence has to be considered as well. The study area has great potential for further investigations concerning climate change, sea level change and tectonic evolution, and settlement history.

## Acknowledgments

This research originated from cooperation between the Institute for Ocean Management, Anna University, Chennai, India, LEUPHANA University Lüneburg and Leibniz-Institute for Applied Geophysics, Hannover, Germany, financed by the German Federal Ministry of Science and Education (BMBF) and by the Indian Department of Science and Technology (DST), which is highly appreciated. We thank Dr. S. Srinivasalu from the Department of Geology, Anna University, Chennai, India for support during fieldwork.

## References

- Achyuthan, H., Baker, V.R., 2002. Coastal response to changes in sea level since the last 4500 BP on the coast of Tamil Nadu, India. *Radiocarbon* 44, 137–144.
- Adamiec, G., Aitken, M., 1998. Dose-rate conversion factors: update. *Ancient TL* 16, 37–50.
- Aitken, M.J., 1998. *An introduction to optical dating*. Oxford University Press, Oxford.
- Arnold, L.J., Bailey, R.M., Tucker, G.E., 2007. Statistical treatment of fluvial dose distributions from southern Colorado arroyo deposits. *Quaternary Geochronology* 2, 162–167.
- Bailey, R.M., Arnold, L.J., 2006. Statistical modelling of single grain quartz  $D_e$  distributions and an assessment of procedures for estimating burial dose. *Quaternary Science Reviews* 25, 2475–2502.
- Ballarini, M., Wallinga, J., Murray, A.S., Heteren, v., S., Oost, A.P., Bos, A.J.J., Eijk, v., C.W.E., 2003. Optical dating of young coastal dunes on a decadal time scale. *Quaternary Science Reviews* 22, 1011–1017.
- Banerjee, P.K., 2000. Holocene and Late Pleistocene relative sea level fluctuations along the east coast of India. *Marine Geology* 167, 243–260.
- Bateman, M.D., 2008. Luminescence dating of periglacial sediments and structures. *Boreas* 37, 574–588.
- Bateman, M.D., Holmes, P.J., Carr, A.S., Horton, B.P., Jaiswal, M.K., 2004. Aeolianite and barrier dune construction spanning the last two glacial-interglacial cycles from the southern Cape coast, South Africa. *Quaternary Science Reviews* 23, 1681–1698.
- Begley, V., 1996. *The ancient port of Arikamedu*. New Excavations and Researches 1989–1992, vol. 1. Paris.
- Berger, G.W., Murray, A.S., Havholm, K.G., 2003. Photonic dating of Holocene back-barrier coastal dunes, northern North Carolina, USA. *Quaternary Science Reviews* 22, 1043–1050.
- Berndtsson, R., Chen, H., 1994. Variability of soil water content along a transect in a desert area. *Journal of Arid Environments* 27, 127–139.
- Berndtsson, R., Nodomi, K., Yasuda, H., Persson, T., Chen, H., Jinno, K., 1996. Soil water and temperature patterns in an arid desert dune sand. *Journal of Hydrology* 185, 221–240.

- Brückner, H., 1988. Indicators for formerly higher sea levels along the east coast of India and on the Andaman Islands. In: *Neue Ergebnisse der Küstenforschung*. K. Schipull, and D. Thannheiser, Eds., pp. 47–72. Hamburger Geographische Studien. Institut für Geographie und Wirtschaftsgeographie der Universität Hamburg, Hamburg.
- Chandrasekharan, S., Murugan, C., 2001. Heavy minerals in the beach and the coastal red sands (Teris) of Tamil Nadu. *Exploration and Research for Atomic Minerals* 13, 87–109.
- Chase, B.M., Thomas, D.S.G., 2007. Multiphase late Quaternary aeolian sediment accumulation in western South Africa: timing and relationship to palaeo-climatic changes inferred from the marine record. *Quaternary International* 166, 29–41.
- Chawla, S., Dhir, R.P., Singhvi, A.K., 1992. Thermoluminescence chronology of sand profiles in the Thar desert and their implications. *Quaternary Science Reviews* 11, 25–32.
- Dhar, O.N., Rakhecha, P.R., Kulkarni, A.K., 1982. Fluctuations in northeast monsoon rainfall of Tamil Nadu. *Journal of Climatology* 2, 339–345.
- Dincer, T., Al-Mugrin, A., Zimmermann, U., 1974. Study of the infiltration and recharge through the sand dunes in arid zones with special reference to the stable isotopes and thermonuclear tritium. *Journal of Hydrology* 23, 79–109.
- Duller, G.A.T., 2003. Distinguishing quartz and feldspar in single grain luminescence measurements. *Radiation Measurements* 37, 161–165.
- Ensign, K.L., Webb, E.A., Longstaffe, F.J., 2006. Microenvironmental and seasonal variations in soil water content of the unsaturated zone of a sand dune system at Pinery Provincial Park, Ontario, Canada. *Geoderma* 136, 788–802.
- Fitzsimmons, K.E., Rhodes, E.J., Magee, J.W., Barrows, T.T., 2007. The timing of linear dune activity in the Strzelecki and Tirari Deserts, Australia. *Quaternary Science Reviews* 26, 2598–2616.
- Fuchs, M., Owen, L.A., 2008. Luminescence dating of glacial and associated sediments: review, recommendations and future directions. *Boreas* 37, 636–659.
- Galbraith, R.F., Roberts, R.G., Laslett, G.M., Yoshida, H., Olley, J.M., 1999. Optical dating of single and multiple grains of quartz from Jinmium Rock Shelter, northern Australia: Part 1, experimental design and statistical models. *Archaeometry* 41, 339–364.
- Gregory, S., 1989. Macro-regional definition and characteristics of Indian summer monsoon rainfall, 1871–1985. *International Journal of Climatology* 9, 465–483.
- Hesse, P.P., Magee, J.W., Kaars v. d., S., 2004. Late Quaternary climates of the Australian arid zone: a review. *Quaternary International* 118–119, 87–102.
- Hilgers, A., Murray, A.S., Schlaak, N., Radtke, U., 2001. Comparison of quartz OSL protocols using Lateglacial and Holocene dune sands from Brandenburg, Germany. *Quaternary Science Reviews* 20, 731–736.
- Holmes, P.J., Bateman, M.D., Thomas, D.S.G., Telfer, M.W., Barker, C.H., Lawson, M.P., 2008. A Holocene-late Pleistocene aeolian record from lunette dunes of the western Free State panfield, South Africa. *The Holocene* 18, 1193–1205.
- Jacobs, Z., 2008. Luminescence chronologies for coastal and marine sediments. *Boreas* 37, 508–535.
- Jayappa, K.S., Vijaya Kumar, G.T., 2006. Beach morphological studies in India – a review. *Journal of the Geological Society of India* 68, 874–884.
- Juyal, N., Kar, A., Rajaguru, S.N., Singhvi, A.K., 2003. Luminescence chronology of aeolian deposition during the Late Quaternary on the southern margin of Thar Desert, India. *Quaternary International* 104, 87–98.
- Kale, V.S., 1999. Long-period fluctuations in monsoon floods in the Deccan Peninsula, India. *Journal of the Geological Society of India* 53, 5–15.
- Kale, V.S., Gupta, A., Singhvi, A.K., 2004. Late Pleistocene–Holocene palaeo-hydrology of monsoon Asia. *Journal of the Geological Society of India* 64, 403–417.
- Kale, V.S., Singhvi, A.K., Mishra, P.K., Banerjee, D., 2000. Sedimentary records and luminescence chronology of Late Holocene palaeofloods in the Luni River, Thar Desert, northwest India. *Catena* 40.
- Kocurek, G., Carr, M., Ewing, R., Havholm, K.G., Nagar, Y.C., Singhvi, A.K., 2007. White sands dune field, New Mexico: age, dune dynamics and recent accumulations. *Sedimentary Geology* 197, 313–331.
- Lancaster, N., 2008. Desert dune dynamics and development: insights from luminescence dating. *Boreas* 37, 559–573.
- Li, S.-H., Sun, J.-M., Zhao, H., 2002. Optical dating of dune sands in the northeastern deserts of China. *Palaeogeography, Palaeoclimatology, Palaeoecology* 181, 419–429.
- Liu, K.-b., Yao, Z., Thompson, L.G., 1998. A pollen record of Holocene climatic changes from the Dunde ice cap, Qinghai–Tibetan Plateau. *Geology* 26, 135–138.
- Lomax, J., Hilgers, A., Twidale, C.R., Bourne, J.A., Radtke, U., 2007. Treatment of broad palaeodose distributions in OSL dating of dune sands from the western Murray Basin, South Australia. *Quaternary Geochronology* 2, 51–56.
- Lomax, J., Hilgers, A., Wopfner, H., Grün, R., Twidale, C.R., Radtke, U., 2003. The onset of dune formation in the Strzelecki Desert, South Australia. *Quaternary Science Reviews* 22, 1067–1076.
- Madsen, A.T., Murray, A.S., Andersen, T.J., 2007. Optical Dating of Dune Ridges on Rømø, a Barrier Island on the Wadden Sea, Denmark. *Journal of Coastal Research* 23, 1259–1269.
- Madsen, A.T., Murray, A.S., Andersen, T.J., Pejrup, M., Breuning-Madsen, H., 2005. Optically stimulated luminescence dating of young estuarine sediments: a comparison with <sup>210</sup>Pb and <sup>137</sup>Cs dating. *Marine Geology* 214, 251–268.
- Mills, P.C., 1983. Genesis and diagnostic value of soft-sediment deformation structures – a review. *Sedimentary Geology* 35, 83–104.
- Mohan, P.M., 1995. Distribution of heavy minerals in Parangipettai (Porto Novo) Beach, Tamil Nadu. *Journal of the Geological Society of India* 46, 401–408.
- Mohan, P.M., Rajamanickam, G.V., 2000. Buried placer mineral deposits along the east coast between Chennai and Pondicherry. *Journal of the Geological Society of India* 56, 1–13.
- Mooley, D.A., Parthasarathy, B., 1983. Droughts and floods over India in summer monsoon seasons 1871–1980. In: *Street-Perrott, A., Beran, M., Ratcliffe, R. (Eds.), Variations in the Global Water Budget*. D. Reidel Publishing Company, Dordrecht, pp. 239–252.
- Mooley, D.A., Parthasarathy, B., 1984. Fluctuations in all-India summer monsoon rainfall during 1871–1978. *Climatic Change* 6, 287–301.
- Munyikwa, K., 2005. The role of dune morphogenetic history in the interpretation of linear dune luminescence chronologies: a review of linear dune dynamics. *Progress in Physical Geography* 29, 317–336.
- Murray-Wallace, C.V., Banerjee, D., Bourman, R.P., Olley, J.M., Brooke, B.P., 2002. Optically stimulated luminescence dating of Holocene relict foredunes, Guichen Bay, South Australia. *Quaternary Science Reviews* 21, 1077–1086.
- Murray, A.S., Olley, J.M., 2002. Precision and accuracy in the optically stimulated luminescence dating of sedimentary quartz: a status review. *Geochronometria* 21, 1–16.
- Murray, A.S., Wintle, A.G., 2000. Luminescence dating of quartz using an improved single-aliquot regenerative-dose protocol. *Radiation Measurements* 32, 57–73.
- Murray, A.S., Wintle, A.G., 2003. The single aliquot regenerative dose protocol: potential for improvements in reliability. *Radiation Measurements* 37, 377–381.
- Neuwerth, R., Suter, F., Guzman, C.A., Gorin, G.E., 2006. Soft-sediment deformation in a tectonically active area: the Plio-Pleistocene Zarzal Formation in the Cauca Valley (Western Colombia). *Sedimentary Geology* 186, 67–88.
- Nigam, R., Khare, N., 1994. Signals of the change in monsoonal precipitation at around 2,000 years BP in a sediment core off central west coast of India. *Current Science* 66, 226–228.
- O'Connor, P.W., Thomas, D.S.G., 1999. The Timing and environmental significance of late quaternary linear dune development in Western Zambia. *Quaternary Research* 52, 44–55.
- Olley, J.M., Murray, A., Roberts, R.G., 1996. The effects of disequilibria in the uranium and thorium decay chains on burial dose rates in fluvial sediments. *Quaternary Science Reviews* 15, 751–760.
- Owen, G., 2003. Load structures: gravity-driven sediment mobilization in the shallow subsurface. *Geological Society Special Publication* 216, 21–34.
- Prasad, S., Enzel, Y., 2006. Holocene paleoclimates of India. *Quaternary Research* 66, 442–453.
- Prescott, J.R., Hutton, J.T., 1994. Cosmic ray contributions to dose rates for luminescence and ESR dating: large depths and long-term time variations. *Radiation Measurements* 23, 497–500.
- Prescott, J.R., Stephan, L.G., 1982. The contribution of cosmic radiation to the environmental dose for thermoluminescent dating – latitude, altitude and depth dependences. *PACT* 6, 17–25.
- Radies, D., Preusser, F., Matter, A., Mange, M., 2004. Eustatic and climatic controls on the development of the Wahiba Sand Sea, Sultanate of Oman. *Sedimentology* 51, 1359–1385.
- Ramasamy, S.M., 2006. Holocene tectonics revealed by Tamil Nadu deltas, India. *Journal of the Geological Society of India* 67, 637–648.
- Ramasamy, S.M., Saravanavel, J., Selvakumar, R., 2006. Late Holocene geomorphic evolution of Cauvery delta, Tamil Nadu. *Journal of the Geological Society of India* 67, 649–657.
- Ramaswamy, K., Duraiswamy, D., 1990. Archaeomagnetic studies on some archaeological sites in Tamil Nadu, India. *Physics of the Earth and Planetary Interiors* 60, 278–284.
- Raval, U., 2002. Is there a major geodynamic node near Pondicherry, the site of 25th September, 2001 earthquake? *Journal of the Geological Society of India* 60, 217–221.
- Ritsema, C.J., Dekker, L.W., 1994. Soil moisture and dry bulk density patterns in bare dune sands. *Journal of Hydrology* 154, 107–131.
- Rittenour, T.M., 2008. Luminescence dating of fluvial deposits: applications to geomorphic, palaeoseismic and archaeological research. *Boreas* 37, 613–635.
- Roberts, H.M., 2008. The development and application of luminescence dating to loess deposits: a perspective on the past, present and future. *Boreas* 37, 483–507.
- Rodnight, H., Duller, G.A.T., Wintle, A.G., Tooth, S., 2006. Assessing the reproducibility and accuracy of optical dating of fluvial deposits. *Quaternary Geochronology* 1, 109–120.
- Siddall, M., Chappell, J., Potter, E.-K., 2007. Eustatic sea level during past interglacials. Developments in Quaternary science. In: Sirocko, F., Clausen, M., Sánchez Goni, M.F., Litt, T. (Eds.), *The climate of past interglacials*. Elsevier, Amsterdam, pp. 75–92.
- Singhvi, A.K., Banerjee, D., Rajaguru, S.N., Kishan Kumar, V.S., 1994. Luminescence chronology of a fossil dune at Budha Pushkar, Thar Desert: Palaeo-environmental and archaeological implications. *Current Science* 66, 770–773.
- Singhvi, A.K., Porat, N., 2008. Impact of luminescence dating on geomorphological and palaeoclimate research in drylands. *Boreas* 37, 536–558.
- Singhvi, A.K., Sharma, Y.P., Agrawal, D.P., 1982. Thermoluminescence dating of sand dunes in Rajasthan. *Nature* 295, 313–315.
- Sun, J., 2000. Origin of eolian sand mobilization during the past 2300 years in the Mu Us Desert, China. *Quaternary Research* 53, 78–88.
- Sun, J., Li, S.-H., Han, P., Chen, Y., 2006. Holocene environmental changes in the central Inner Mongolia, based on single-aliquot-quartz optical dating and

- multi-proxy study of dune sands. *Palaeogeography, Palaeoclimatology, Palaeoecology* 233, 51–62.
- Tchakerian, V.P., Lancaster, N., 2002. Late Quaternary arid/humid cycles in the Mojave Desert and western Great Basin of North America. *Quaternary Science Reviews* 21, 799–810.
- Telfer, M.W., Thomas, D.S.G., 2007. Late Quaternary linear dune accumulation and chronostratigraphy of the southwestern Kalahari: implications for aeolian palaeoclimatic reconstructions and predictions of future dynamics. *Quaternary Science Reviews* 26, 2617–2630.
- Thomas, J.V., Kar, A., Kailath, A.J., Juyal, N., Rajaguru, S.N., Singhvi, A.K., 1999. Late Pleistocene–Holocene history of aeolian accumulation in the Thar Desert, India. *Zeitschrift für Geomorphologie Supplementband* 116, 181–194.
- Thomas, P.J., Juyal, N., Kale, V., Singhvi, A.K., 2007. Luminescence chronology of late Holocene extreme hydrological events in the upper Penner River basin, South India. *Journal of Quaternary Science* 22, 747–753.
- Thompson, L.G., Yao, T., Mosley-Thompson, E., Davis, M.E., Henderson, K.A., Lin, P.-N., 2000. A high-resolution millennial record of the south Asian Monsoon from Himalayan ice cores. *Science* 289, 1916–1919.
- Twidale, C.R., Bourne, J.A., Spooner, N.A., Rhodes, E.J., 2007. The age of the palaeodune field of the northern Murray Basin in South Australia: preliminary results. *Quaternary International* 166, 42–48.
- Ujházy, K., Gábris, G., Frechen, M., 2003. Ages of periods of sand movement in Hungary determined through luminescence measurements. *Quaternary International* 111, 91–100.
- Verhoeven, R., 2002. The structure of the microtrophic system in a development series of dune soils. *Pedobiologia* 46, 75–89.
- Walsh, R.P.D., Glaser, R., Militzer, S., 1999. The climate of Madras during the eighteenth century. *International Journal of Climatology* 19, 1025–1047.
- Wintle, A.G., Murray, A.S., 2006. A review of quartz optically stimulated luminescence characteristics and their relevance in single-aliquot regeneration dating protocols. *Radiation Measurements* 41, 369–391.
- Wolfe, S.A., Huntley, D.J., David, P.P., Ollerhead, J., Sauchyn, D.J., MacDonald, G.M., 2001. Late 18th century drought-induced sand dune activity, Great Sand Hills, Saskatchewan. *Canadian Journal of Earth Sciences* 38, 105–117.
- Zander, A.M., 2000. Vergleich verschiedener Lumineszenzmethoden zur Datierung von Löss. *Kölner Forum für Geologie und Paläontologie* 6, 1–92.